LAWRENCE
LIVERMORE
NATIONAL
LABORATORY

LLNL-CONF-407188

Development, characterization and experimental performance of x-ray optics for the LCLS free-electron laser

R. Soufli, M. J. Pivovaroff, S. L. Baker, J. C. Robinson, E. M. Gullikson, T. J. Mc Carville, P. M. Stefan, A. L. Aquila, J. Ayers, M. A. McKernan, R. M. Bionta

September 23, 2008

Advances in X-Ray/EUV Optics and Components III, part of SPIE's Optics and Photonics Meeting
San Diego, CA, United States
August 10, 2008 through August 14, 2008

Disclaimer

Development, characterization and experimental performance of x-ray optics for the LCLS free-electron laser

Regina Soufli[1*], Michael J. Pivovaroff[1], Sherry L. Baker[1], Jeff C. Robinson[1], Eric M. Gullikson[2], Tom J. McCarville[1], Peter M. Stefan[3], Andrew L. Aquila[2], Jay Ayers[1], Mark A. McKernan[1], Richard M. Bionta[1]

[1]Lawrence Livermore National Laboratory, 7000 East Avenue, Livermore, CA 94550, US
[2]Lawrence Berkeley National Laboratory, 1 Cyclotron Road, Berkeley, CA 94720, US
[3]Stanford Linear Accelerator Center, 2575 Sand Hill Road, Menlo Park, CA 94025, US

ABSTRACT

This manuscript discusses the development of reflective optics for the x-ray offset mirror systems of the Linac Coherent Light Source (LCLS), a 0.15−1.5 nm free-electron laser (FEL) at the Stanford Linear Accelerator Center (SLAC). The unique properties (such as the high peak brightness) of the LCLS FEL beam translate to strict limits in terms of materials choice, thus leading to an x-ray mirror design consisting of a reflective coating deposited on a silicon substrate. Furthermore, the physics requirements for these mirrors result in stringent surface figure and finish specifications that challenge the state-of-the-art in x-ray substrate manufacturing, thin film deposition, and metrology capabilities. Recent experimental results on the development, optimization, and characterization of the LCLS soft x-ray mirrors are presented in this manuscript, including: precision surface metrology on the silicon substrates, and the development of boron carbide reflective coatings with reduced stress and thickness variation < 0.14 nm rms across the 175-mm clear aperture area of the LCLS soft x-ray mirrors.

Keywords: free-electron lasers, x-ray optics, boron carbide

1. INTRODUCTION

There are several next-generation synchrotron and free-electron laser (FEL) facilities currently under construction around the world. The unprecedented brightness, coherence, and resolution properties of these sources will enable tremendous advances in the fields of biology, physics, and materials sciences. The Linac Coherent Light Source (LCLS) FEL is currently being installed at the Stanford Linear Accelerator Center (SLAC), is anticipated to begin operation in 2009, and will be the first x-ray FEL facility in the world in the 0.827 to 8.27 keV photon energy region (0.15 − 1.5 nm wavelength region). The experimental areas planned for the LCLS, each with its own dedicated end-station (hutch), include: soft x-ray research (SXR); atomic, molecular and optical science (AMO); x-ray pump-probe (XPP); x-ray photon correlation spectroscopy (XPCS); coherent x-ray imaging (CXI); and high-energy density science (HED)[1]. The layout of the LCLS facility, including the experimental end-stations, has been discussed in detail in an earlier SPIE Proceedings publication[2]. The LCLS x-ray mirror systems serve two distinct purposes. The first is to dramatically reduce the amount of high-energy spontaneous radiation, bremsstrahlung γ-rays and their secondary products within the experimental hutches. The second is to physically separate the FEL beam from the spontaneous, broad-band undulator radiation that would contaminate the spectrally-pure, coherent FEL radiation. An elegant method for achieving the desired goals relies on grazing-incidence mirrors to act as a low-pass energy filter, efficiently reflecting and deflecting the FEL beam to a trajectory slightly offset from the primary axis of the LCLS facility. To minimize costs associated with translating experiments out of the FEL path, allowing the FEL beam to pass to another hutch further down stream, the LCLS x-ray mirror system is designed to provide several different branch lines. The initial LCLS configuration will contain three "lines" by using a combination of fixed and moveable reflective mirrors and splitting the 0.827−8.27 keV first-harmonic range into two regimes: a 0.827−2.00 keV soft x-ray band and a 2.00−8.27 keV hard x-ray band. As has been described in detail in Ref. 2, a total of four mirrors will create two soft x-ray branches that will deliver X-rays to the

* e-mail: regina.soufli@llnl.gov, phone: 925-422-6013

SXR and AMO hutches. Two additional mirrors will create the single hard x-ray branch line that will initially deliver photons to the XPP and CXI hutches. The remainder of this manuscript focuses on the development of optics for the Soft X-ray Mirror Offset System (SOMS) that provides the two branch lines for the SXR and AMO experiments. The Hard X-ray Mirror Offset System (HOMS), designated to deliver photons to the XPP and CXI experiments, will be discussed in a future publication.

2. PHYSICS REQUIREMENTS AND SPECIFICATIONS

2.1 LCLS physics requirements and mirror substrate specifications

The LCLS physics requirements that drive the specifications for the SOMS mirrors have been discussed in detail in Ref. 2 (and references therein) and are summarized below:

1. *Reflective materials specifications:* One of the most unique LCLS beam properties is the extremely high peak brightness (~ 10^{32} photons*sec^{-1}*mm^{-2}*mrad^{-2} *(0.1% bandwidth)$^{-1}$), which is over ten orders of magnitude higher than current third-generation synchrotron sources. Earlier studies[3,4,5,6] indicate that only a few low-Z materials (Be, B_4C, SiC and Al_2O_3) would be expected to survive the peak brightness of the LCLS FEL beam after it leaves the undulator enclosure. In addition, there is a requirement for absence of absorption edges in the photon energy range of operation (0.827−2.00 keV for the SOMS mirrors), to ease the calibration of reflectivity data obtained from the SOMS mirrors.
2. *3rd harmonic rejection:* The reflectance of each SOMS mirror at photon energies above 2.48 keV should be less than 20%.
3. *Mirror reflectance:* Each SOMS mirror should have reflectivity ≥ 90% in the entire SOMS photon energy range at the SOMS grazing angle of incidence of 13.85 mrad (0.79 degrees).
4. *Mirror geometry:* The SOMS mirrors will have flat, planar reflective surfaces
5. *Mirror acceptance:* Each SOMS mirror should be sized to accept at least 95% of the FEL beam radiation cone.
6. *Mirror surface specifications:* Each SOMS mirror surface should be specified to limit degradation of the transverse coherence of the FEL beam. In addition, each SOMS mirror should not reduce the FEL beam intensity by more than 20% or broaden its divergence by more than 10%.

Requirements no. 1, 2 and 3 above, combined with the state-of-the-art in vendor capabilities to polish/figure specific materials, resulted in a design for the SOMS mirrors consisting of a Si substrate followed by a 50-nm thick B_4C reflective coating. Requirements no. 4, 5, 6 above, resulted in the surface figure, mid-spatial frequency roughness (MSFR) and high-spatial frequency roughness (HSFR) specifications summarized in Table 1. The size of the SOMS mirror was defined as 250 mm (length)×30 mm (width) ×50 mm (height), with a clear aperture (illuminated area required to meet surface specifications) of 175mm ×10 mm. The slope and height error specifications in Table 1 apply to the tangential direction, after subtraction of any spherical-term figure error component. The slope and height error specifications for the surface figure are especially crucial in meeting the requirements for coherence preservation of the LCLS FEL beam. Achieving the surface specifications for the mirror substrate figure and finish in Table 1 is a daunting task and is truly pushing the limits of the state-of-the-art in Si substrate manufacturing and metrology. A schematic drawing of the top (reflecting) surface of the SOMS mirror substrate, illustrating the clear aperture, is shown in Fig. 1. The mounting design and other opto-mechanical and thermal considerations for the SOMS mirrors are discussed in detail in Ref. 7 in this Conference Proceedings.

Error Category		Specification	Spatial Wavelength
Figure	Height Error	≤ 2.0 nm rms	1 mm to Clear Aperture
	Slope Error	≤ 0.25 μrad rms	
MSFR		≤ 0.25 nm rms	2 μm to 1 mm
HSFR		≤ 0.4 nm rms	20 nm to 2 μm

Table 1: Surface specifications for the figure, MSFR and HSFR of the SOMS Si substrates. All specifications are applicable within the substrate clear aperture area, 175mm × 10 mm.

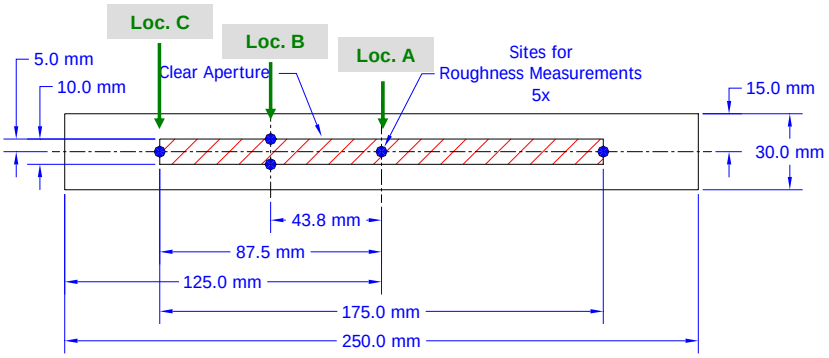

Figure 1: Schematic drawing of the top surface of the SOMS mirror substrate, with the clear aperture shown as a shaded area. Locations A, B, C, where precision metrology results are discussed in Section 3 of this manuscript, are also shown.

2.2 Reflective coating specifications

One of the most important requirements for the 50 nm-thick B_4C reflective coating for the LCLS SOMS mirrors is to preserve the figure of the Si substrate specified in Table 1. Given that the figure errors of the substrate and subsequent reflective coating are uncorrelated and thus add in a quadratic fashion, the thickness variation of the B_4C film should be < 1 nm rms (i.e: about half of the substrate figure specification) across the 175 mm mirror clear aperture, in order for the B_4C coating thickness variation to not have a significant contribution to degradation of the mirror figure. Moreover, the coating is required to preserve the MSFR of the Si substrate specified in Table 1. The coating contribution to HSFR should allow for about ≥ 90% reflectance per mirror, as is specified in Section 2.1. The stress of the B_4C coating should be sufficiently low (~ 1 GPa or less, for a 50-nm thick coating) to prevent delamination from the substrate and maintain the overall figure deformation of the B_4C -coated mirror within the specification of 2 nm rms. As is the case with all reflective coatings for x-ray optics, the top surface of the B_4C film should be stable against contamination (oxidation, hydrocarbons), to maintain consistent reflective performance over time. Experimental results addressing all the above specifications are presented in Section 4 of this manuscript.

3. SUBSTRATE METROLOGY FOR THE LCLS SOFT X-RAY MIRRORS

It is essential to accurately measure the surface topography of an x-ray optical substrate in the low (figure), mid- and high-spatial frequency ranges and compare the results against the specifications, in order to understand and interpret correctly the reflective performance of the optic. Especially in the case of the SOMS substrates, given the very challenging specifications discussed in Section 2.1 and Table 1 and their predicted impact on mirror performance, precision surface metrology is a crucial part of the substrate acceptance process. Precision surface metrology was performed at Lawrence Livermore National Lab (LLNL) on a recently delivered SOMS Si substrate, manufactured by InSync, Inc. (Albuquerque, New Mexico). High-spatial frequencies were measured with a Digital Instruments Dimension 5000™ Atomic Force Microscope (AFM), equipped with an acoustic hood and vibration isolation, resulting in a noise level of 0.03 nm rms. The instrument is operated in tapping mode which measures topography in air by tapping the surface with an oscillating probe tip. The probe tips were etched silicon, with a nominal tip radius of 5-10 nm. AFM scans of 2×2 μm^2 and 10×10 μm^2 were performed and the data from each scan were stored in a 512×512 pixel array. Mid-spatial frequencies were measured using a Zygo New View™ phase-profiling optical microscope. Scans were performed with two objective lens magnifications, 2× and 20×, on each location and the data from each scan were stored in a 640×480 pixel array. AFM and Zygo measurements were obtained on three locations within the substrate clear aperture, shown in Fig. 1, and images from one of the measured locations are shown in Figures 2 and 3. The power spectral density (PSD) was computed[8] from the height data in each of the AFM and Zygo scans. The PSD was formed by first calculating a two-dimensional Fourier power spectrum of the height data, and the spectrum was then averaged azimuthally around zero spatial frequency to produce a PSD with purely radial spatial frequency dependence. This approach works well for quasi-isotropic surfaces, such as the substrate surface shown in Figures 2 and 3. The PSD curves obtained from AFM and Zygo measurements on the 3 locations, covering the area from the center to the edge of the clear aperture of the SOMS mirror substrate, are shown in Fig. 4. The PSD curves among the 3 locations overlap very well, indicating an optical surface with uniform finish. Furthermore, there is excellent overlap between the PSD curves

from the Zygo and AFM instruments and between the different magnifications from a given instrument, which provides further confidence and validation of our metrology and analysis processes. The root-mean-square (rms) roughness σ is obtained by the expression

$$\sigma^2 = \int_{f_1}^{f_2} 2\pi f S(f) df \quad , \qquad (1)$$

where f is the spatial frequency, $S(f)$ is the surface PSD, and f_1, f_2 define the spatial frequency range of interest. For the HSFR, where $f_1 = 5\times10^{-4}$ nm^{-1} and $f_2 = 5\times10^{-2}$ nm^{-1} as defined in Table 1, σ was computed according to eq. (1) by combining PSD curves from 10×10 μm^2 and 2×2 μm^2 AFM scans. For the MSFR, where $f_1 = 10^{-6}$ nm^{-1} and $f_2 = 5\times10^{-4}$ nm^{-1} as defined in Table 1, σ was computed according to eq. (1) by combining PSD curves from 2× and 20× Zygo magnifications and 10×10 μm^2 AFM scans. The rms HSFR and MSFR (σ) values computed in this manner are listed in Table 2 for each of the 3 locations measured. HSFR values are within specification, while MSFR values are somewhat missing the specification. The increased MSFR is expected to lead to increased scattering on the "wings" of the LCLS beam. This SOMS substrate was nevertheless accepted by LLNL, as this effect was not considered significantly detrimental to the LCLS FEL beam properties. We are currently in the process of modeling the effects of substrate surface errors on the LCLS FEL beam wavefront, and will discuss this topic in detail in a future publication.

The surface figure of the SOMS Si substrate is currently being measured by full-aperture interferometry at LLNL, using a Zygo Mark II^{TM}, 12"-diameter phase-shifting Fizeau-type interferometer with an accuracy of ± 2 nm (3σ confidence interval) operating at the He-Ne wavelength of 633 nm. A calibrated transmission flat is used as a reference surface. The interferometry measurements and analysis on this SOMS substrate indicate that the figure and slope errors within the clear aperture are 1.9 nm rms and 0.15 μrad rms, which meet the figure specifications set in Table 1 for the SOMS Si substrates.

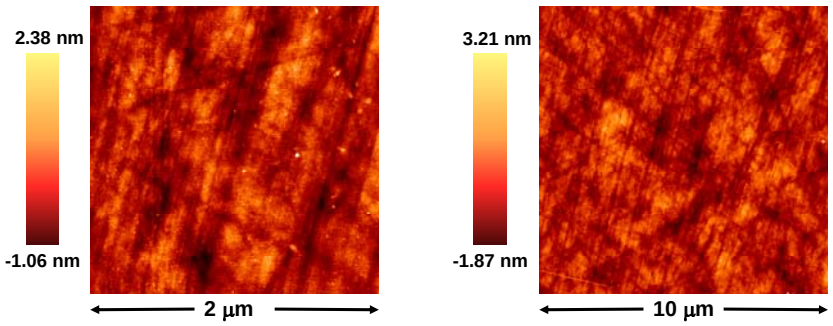

Figure 2: AFM images obtained on one of the surface locations (loc. C) of the SOMS Si substrate, shown in Figure 1.

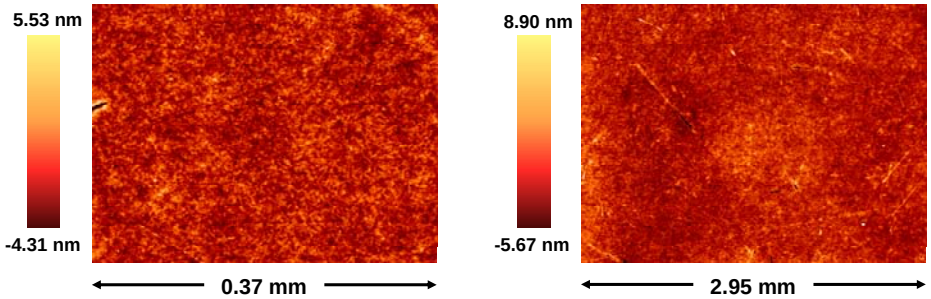

Figure 3: Zygo phase profiling microscope images, using 20X (left) and 2X (right) magnifications, obtained on one of the surface locations (loc. C, shown in Fig. 1) of the SOMS Si substrate.

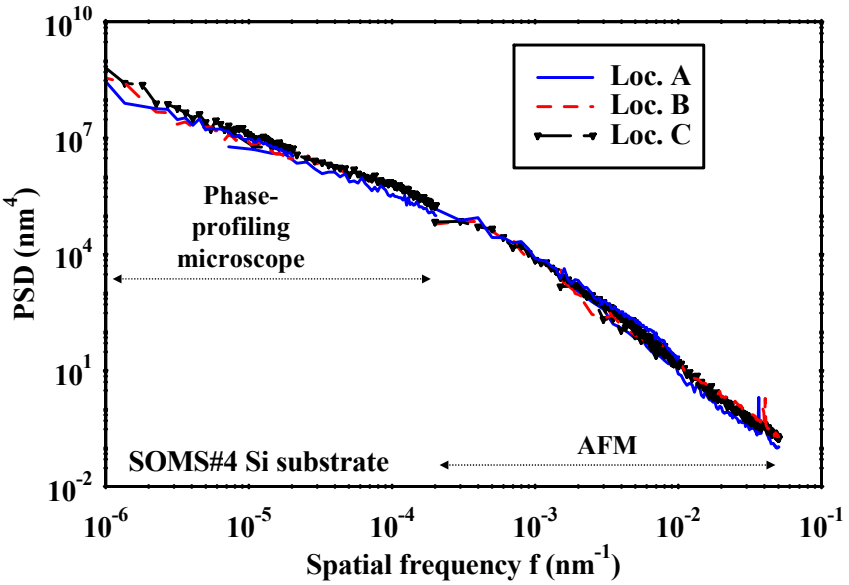

Figure 4: PSD curves in the MSFR and HSFR range for one of the SOMS Si substrates, derived from precision surface metrology on 3 locations (shown in Fig. 1).

	Spatial Frequency Range	Spatial Wavelength Range	SOMS Specification	SOMS#4, measured
HSFR	0.5 μm^{-1} - 50 μm^{-1} 5×10^{-4} nm^{-1} - 5×10^{-2} nm^{-1}	20 nm - 2 µm	≤ 0.4 nm rms	A = 0.30 nm rms B = 0.31 nm rms C = 0.34 nm rms
MSFR	10^{-3} μm^{-1} - 0.5 μm^{-1} 10^{-6} nm^{-1} - 5×10^{-4} nm^{-1}	2 µm - 1 mm	≤ 0.25 nm rms	A = 0.32 nm rms B = 0.37 nm rms C = 0.37 nm rms
Figure	(mirror CA)$^{-1}$ - 10^{-3} μm^{-1}	Mirror CA – 1 mm	≤ 0.25 µrad rms and < 2 nm rms	0.15 µrad rms and 1.9 nm rms

Table 2: Summary of measured rms roughness values for the HSFR, MSFR and figure, for one of the actual SOMS Si substrates. A schematic drawing of locations A, B, C, where the HSFR and MSFR measurements were obtained is shown in Fig. 1.

4. REFLECTIVE COATING DEVELOPMENT FOR THE LCLS SOFT X-RAY MIRRORS

As is discussed in Sections 2.1 and 2.2, B_4C was chosen as the reflective coating material for the LCLS SOMS mirrors mainly due to the predicted high damage threshold against the LCLS FEL beam compared to other coating materials, combined with the good reflective performance and absence of electronic absorption edges in the 0.827-2.00 keV SOMS energy range of operation. For the single-layer, grazing incidence SOMS mirrors of the LCLS, it was determined through modeling that the optimum thickness of the B_4C coating is about 50 nm, to ensure good reflective properties and adequate suppression of the higher harmonics of the FEL beam. In the past 20 years, magnetron or ion-beam sputtered B_4C films with thicknesses ranging from a fraction of a nanometer to a few nanometers have been used as barrier or constituent layers in reflective multilayer optics operating in the extreme ultraviolet (EUV) and x-ray energy region. Although there is significant literature on sputtered boron carbide films tailored for the aforementioned applications,

there is only limited work from earlier studies[9,10,11,12] on the physical and optical properties of single-layer, sputtered B_4C films in the 50-nm thickness range as EUV/x-ray reflective coatings. Specifically in the SOMS photon energy range of operation (0.827-2.00 keV), the experimental reflectivity of grazing incidence x-ray mirrors with such B_4C coatings has not been investigated previously.

To investigate the B_4C coating properties for the SOMS mirror application, B_4C coatings were deposited at LLNL on clean, (100)-orientation Si wafer substrates with nearly ideal HSFR (about 0.05 nm rms). A planar DC-magnetron sputtering system for large-area, ultra-precise EUV/x-ray coatings[13] was used for these depositions. The same system will ultimately be used for the deposition of the B_4C coatings on the actual SOMS mirror substrates. X-ray Photoelectron Spectroscopy (XPS) on samples aged for about one month indicated that the top 9 nm of the films are oxygen- and carbon- rich (boron=64%, carbon= 22%, oxygen=13%, atomic) with the oxygen and carbon concentrations rapidly diminishing with increasing depth from the top surface. Rutherford backscattering (RBS) measurements indicated boron-to-carbon = 3.7 : 1 atomic ratio, with 6% (atomic) oxygen present, averaged across the entire film thickness. The boron-to-carbon ratio is close to the prescribed stoichiometry (4 : 1) of the sputtering target material, and the overall composition (including the oxygen content) is consistent with earlier results reported in the literature for sputtered boron carbide thin films. It was determined that the 6% oxygen in the films is most likely coming from the boron carbide sputtering target (i.e: was incorporated during target fabrication), as opposed to oxygen being present in the environment during deposition. This is further supported by the observation that films of other materials made in the same deposition chamber under similar conditions and tested by RBS show only a fraction of a percent atomic oxygen concentration. Through RBS measurements it was also determined that the density of the sputtered films is 2.28 g/cm^3, which corresponds to 90% of the bulk density of a boron carbide crystal (2.52 g/cm^3). RBS and XPS measurements were performed by Evans Analytical Group (Sunnyvale, California). The HSFR (in the frequency range specified in Table 2) of a 50-nm thick B_4C coating made using nominal deposition parameters was 0.15 nm rms, measured by AFM. The stress of this film was -2.3 GPa (compressive). Although no delamination or other degradation has been observed on several such films aged for over two years after deposition, this level of stress was considered a risk for the actual SOMS mirrors. By especially modifying the deposition parameters, B_4C films with a factor of 2 lower stress (-1.1 GPa) were produced. The stress of the latter films meets the reflective coating requirements discussed in Section 2.2, and has been predicted -and experimentally verified- to induce a figure deformation with a spherical-term-like shape on the SOMS substrate, which can be corrected using a special bending mechanism during final assembly of the SOMS mirrors[7]. The high-spatial frequency roughness of the modified B_4C film was 0.5 nm rms, which was accepted as a trade-off for the lower stress offered by this modified B_4C film. The modified, lower-stress B_4C film with 50 nm thickness was ultimately selected as the reflective coating for the LCLS SOMS mirrors. The refractive index (optical constants) of the modified B_4C films was also determined experimentally via photoabsorption measurements[14]. A detailed discussion of the morphology, microstructure and stress properties of these B_4C coatings will be given in an upcoming publication.

Prior to coating the actual SOMS Si substrates with the lower-stress B_4C coating discussed above, the roughness and reflectivity properties of the B_4C coating (deposited on a non-ideal substrate) were verified on a Si test substrate provided by the manufacturer of the actual SOMS Si substrates, using the same polishing methods as for the actual SOMS substrates. The Si test substrate was a disc of 50 mm-diameter and 9 mm-thickness. The MSFR and HSFR of the Si substrate was measured before and after coating with the 50-nm thick B_4C coating, using the techniques discussed in Section 3, and the measured PSD curves are plotted in Fig. 5. Furthermore, a stochastic thin film growth model formulated for vapor phase deposition processes[15] was used to predict the PSD of the top surface of the B_4C-coated substrate. According to the model, the PSD of the film (PSD^{film}) (deposited on an ideal substrate) is given by the expression

$$PSD^{film}(q) = \Omega \frac{1 - \exp(-2\nu\, d q^n)}{2\nu\, q^n}, \qquad (2)$$

where $q=2\pi f$, Ω represents the sputtered particle volume, ν is related to the lateral distance over which sputtered particles can relax, d is the film thickness and n is an exponential parameter characteristic of the deposition process. During earlier studies[16], n=4 has been established as the characteristic exponent for DC-magnetron sputtering film growth. Given a film with PSD^{film} grown on a substrate with PSD^{sub}, the overall PSD of the top coated surface, (PSD^{top}) is given by

$$PSD^{top} = PSD^{film} + \alpha^2 PSD^{sub}, \qquad (3)$$

where

$$\alpha(q) = \exp(-\nu\, dq^{n}) \qquad (4)$$

is the replication factor from the substrate to the coating. For the present B_4C films, PSD^{top} is calculated in Fig. 5 using equations (2)-(4) with n=4, d = 50 nm, Ω = 1.4 nm^3, ν = 7 nm^3. The values for Ω and ν were experimentally determined by fitting PSD curves obtained from AFM measurements on the 50-nm thick B_4C film (deposited on a Si wafer with near-zero roughness) to eq. (2). The measured PSD of the Si test substrate was implemented in equation (3) as PSD^{sub}. The PSD of the B_4C–coated top surface calculated by the above model is also plotted in Fig. 5. There is good agreement between calculated and measured PSD curves. The calculated PSD predicts correctly the onset spatial frequency where the roughness from the B_4C coating makes its contribution, and also predicts correctly the overall shape of the PSD at the higher spatial frequencies, but somewhat underestimates the HSFR when compared to the measured PSD. This could be attributed to the fact that the roughness of the Si test substrate may be affecting the growth properties of the B_4C film. In the mid-spatial frequency range and in the lower portion of the high-spatial frequency range, Fig.5 shows that the B_4C coating replicates the topography of the Si substrate, as has also been demonstrated on earlier DC-magnetron sputtered coatings of various single-layer and multilayer materials deposited under similar conditions[16,17]. The HSFR, defined in Table 1 and eq. (1) for the SOMS mirrors, is also determined for each of the 3 cases in Fig. 5. The measured HSFR of the Si substrate is 0.36 nm rms and becomes 0.79 nm rms after coating with the 50-nm thick, lower-stress B_4C coating.

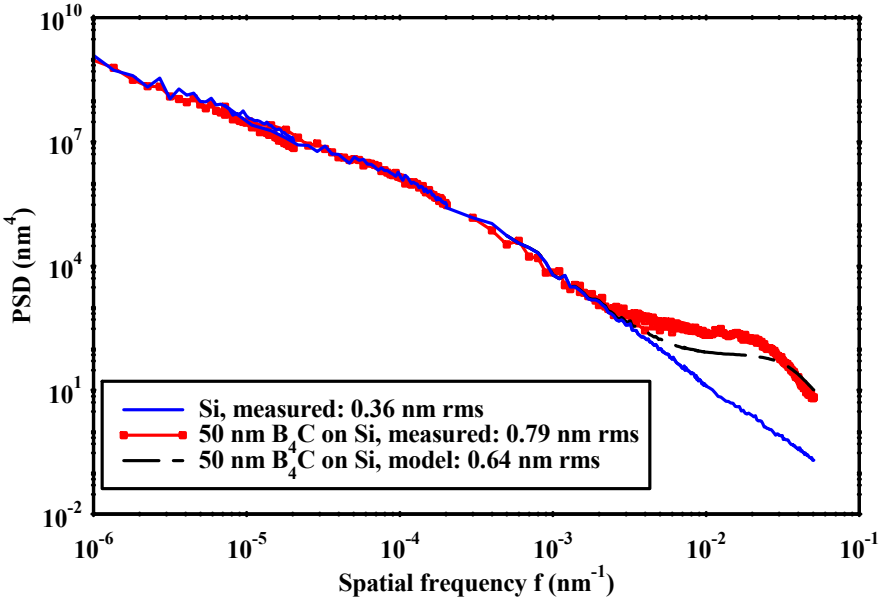

Figure 5: Measured PSD curves and rms HSFR values for a SOMS test Si substrate, before and after coating with 50 nm of a B_4C reflective coating optimized for lower stress for the SOMS mirrors. A stochastic growth thin film model was also used to calculate the PSD of the coated surface, and is shown as a dashed line.

The x-ray reflectance of the B_4C-coated test substrate discussed above was measured at beamline 6.3.2.[18,19] of the Advanced Light Source (ALS) synchrotron at Lawrence Berkeley National Lab. The energy range of the beamline is 30 eV-1.2 keV. In order to verify the reflective performance of the sample at a photon energy within the 0.827-2.00 keV SOMS energy range of operation, a photon energy of 0.9 keV was selected for the reflectance measurements. A wire detector with 1 degree acceptance angle was used. The measured reflectance vs. grazing incidence angle is shown in Fig. 6. The reflectance at the SOMS angle of incidence (0.79 degrees) is 88.4%, which was deemed acceptable since it is very close to the 90% reflectance requirement discussed in Sections 2.1, 2.2, and given that throughput is not a major consideration for the SOMS mirror performance. The reflectance measurement in Fig. 6 was performed 2 days after deposition of the B_4C coating. The same measurement was repeated 3.5 months after deposition, with the sample stored

in ambient environment. The two measurements produced identical reflectance results, which is encouraging for the lifetime stability of this coating.

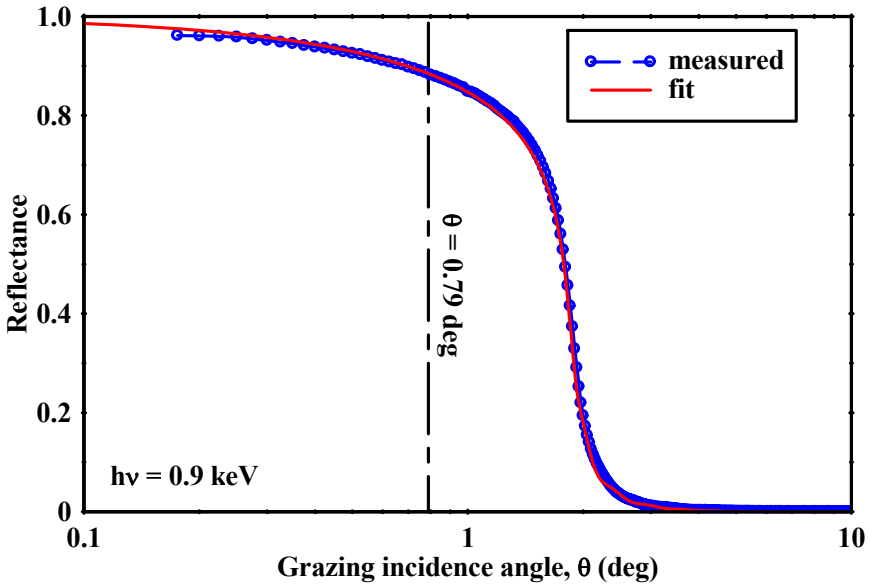

Figure 6: Measured reflectance vs. grazing incidence angle (on a logarithmic axis) of a B_4C-coated, SOMS Si test substrate. The angle of incidence of the SOMS mirrors is marked with a vertical dashed line. A fit[20] to the measured data is also shown, using thickness, density, composition and roughness parameters determined experimentally, as is discussed earlier in the manuscript.

The B_4C coating thickness variation is most crucial to the SOMS mirror performance since it is related to the wavefront (coherence) preservation of the LCLS FEL beam, as is discussed in Sections 2.1, 2.2. In order to optimize the B_4C coating thickness and meet the < 1 nm rms thickness variation requirement (discussed in Section 2.2) across the 175 mm-long SOMS clear aperture, a Si test substrate assembly with identical dimensions to the SOMS substrate was used. The SOMS test substrate is mounted on the deposition platter, which is located below the B_4C sputtering target inside the planar DC-magnetron sputtering tool. During deposition, the platter is passing underneath the target in a rotational motion while at the same time the SOMS substrate is spinning around its center at several hundred rpm to average out any spatial non-uniformities of the B_4C target. In this manner, the B_4C coating thickness variation is always symmetric around the center of the substrate. An algorithm based on modulation of the rotational velocity of the deposition platter, discussed in detail in Ref. 13, was used to control the coating thickness and to achieve the desired uniformity. The velocity modulation method is stable and rapidly converging and has been implemented in the past to coat several sets of diffraction-limited EUV multilayer optics (see Ref. 13 and references therein). The results of each SOMS coating iteration were measured at beamline 6.3.2. of the ALS, using a photodiode detector with 2.4 degrees acceptance. The SOMS thickness specification was met after a few iterations. The results of the final B_4C coating iteration for SOMS are shown in Fig. 7. The B_4C coating thickness was first verified at three locations on the mirror (y = 30, 50, and 90 mm), by measuring reflectance vs. grazing incidence angle on each location at 91.8 eV photon energy, and by fitting the Kiessig interference fringes as shown in Fig. 7 (top). The y-direction was set to coincide with the center line of the SOMS mirror in the tangential direction (shown as a dash-dot line in Fig. 1), with y = 0 being the center of the SOMS mirror. Given that the coating thickness variation is symmetric around the center of the SOMS mirror as explained above, and the SOMS clear aperture extends from y = -87.5 mm to y = 87.5 mm, only data for positive y values are plotted in Fig.7. The B_4C coating thickness on all three locations was found to be 50.5 ± 0.2 nm, where ± 0.2 nm is the sensitivity of the fitting method to coating thickness variation. Furthermore, the reflectance vs. position (y) was measured at two fixed grazing incidence angles (22.5 and 37 degrees) at 91.8 eV, as shown in Fig. 7 (bottom). Each of the two incidence angles was chosen to be located on an area of a Kiessig fringe that would be most sensitive to coating thickness variation. The measurements shown in Fig.7 (bottom) demonstrate that the coating thickness remains within 50.5 ± 0.2 nm across the SOMS clear aperture, thus demonstrating thickness variation < 0.4 nm peak-to-valley, equivalent to < 0.14 nm rms or

0.28% rms for the 50.5 nm-thick coating. This result is well within the < 1 nm rms specification set for the SOMS B_4C coatings in Section 2.2, thus ensuring that the B_4C coating will not affect the wavefront (coherence) of the LCLS FEL beam. It should be noted that the reflectance variation seen for y >50 mm in Fig. 7 (bottom) is mostly attributed to spatial non-uniformity of the photodiode detector, rather than variation of the B_4C coating thickness.

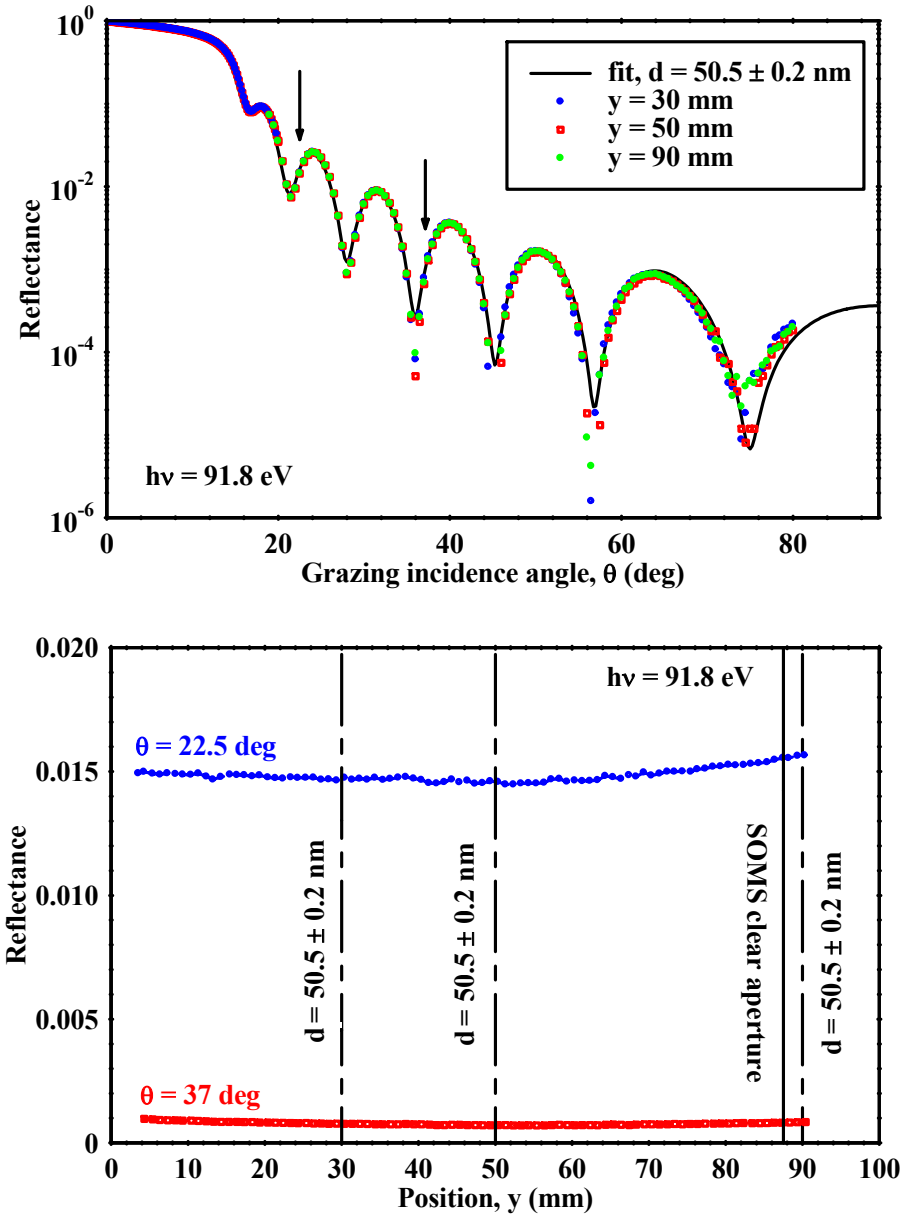

Figure 7: Top: EUV reflectance measurements vs. grazing incidence angle at 3 locations (y = 30, 50, 90 mm) across the center line of the SOMS test mirror, used to verify the B_4C coating thickness. The fitted[20] thickness was d = 50.5 ± 0.2 nm at all three locations. **Bottom:** EUV reflectance measurements vs. y location at two fixed angles of incidence (noted by arrows in the top plot), used to verify the B_4C coating thickness variation across the SOMS mirror. The 3 locations measured in the top plot are shown as vertical dashed lines, and the edge of the SOMS clear aperture is shown as a vertical solid line.

4. SUMMARY AND FUTURE WORK

The SOMS, operating in the photon energy range 0.827-2.00 keV, is the first x-ray mirror system that will encounter the LCLS FEL beam after it leaves the undulator enclosure and is thus subject to a set of unique LCLS physics requirements and specifications. A design consisting of a Si substrate followed by a 50-nm thick B_4C reflective coating was developed at LLNL for the SOMS mirrors. Precision surface metrology and a suite of other characterization techniques (such as RBS, XPS and EUV/x-ray reflectance measurements), as well as a stochastic thin film growth model, were employed to demonstrate experimentally that the B_4C-coated SOMS mirrors will meet the very stringent LCLS requirements. A thickness variation of < 0.14 nm rms across the 175 mm SOMS clear aperture was demonstrated for the B_4C coating, well within the 1 nm rms specification. Delivery of the SOMS Si substrates by the vendor and precision surface metrology at LLNL are currently in progress. Following the acceptance of each SOMS Si substrate, the B_4C reflective coating will be deposited at LLNL as discussed in this manuscript. We have ongoing research towards better understanding of thin film and mirror substrate properties under peak power FEL conditions. We are also in the process of incorporating precision metrology results from mirrors into wavefront propagation models for the LCLS beam. We will report on these results in upcoming publications.

ACKNOWLEDGEMENTS

We are grateful to Donn McMahon (LLNL) for project management support. We thank Angela Craig, Bruce Rothman and Patrick Schnabel (Evans Analytical Group, Sunnyvale, California) for the XPS and RBS measurements. This work performed under the auspices of the U.S. Department of Energy by Lawrence Livermore National Laboratory under Contract DE-AC52-07NA27344. Work was supported in part by DOE Contract DE-AC02-76SF00515. This work was performed in support of the LCLS project at SLAC.

REFERENCES

[1] The LCLS Design Study Group, "Linac coherent light source (LCLS) design study report." SLAC-R-521; UC-414; http://www-ssrl.slac.stanford.edu/lcls/design report/e-toc.html, December 1998.
[2] M. Pivovaroff, R. M. Bionta, T. J. Mccarville, R. Soufli, P. M. Stefan, "Soft X-ray mirrors for the Linac Coherent Light Source", Proc. SPIE **6705**, 67050O (2007).
[3] R. M. Bionta, "Controlling dose to low-Z solids at LCLS." LLNL report: UCRL-ID-137222; http://www.llnl.gov/tid/lof/documents/pdf/237970.pdf , Jan 2000.
[4] D. D. Ryutov, "Thermal stresses in the reflective x-ray optics for the linac coherent light source," *Rev Sci Inst* **74**, 3722–3725 (2003).
[5] S. Hau-Riege, "Absorbed XFEL dose in the components of the LCLS X-Ray optics." LLNL report: UCRLTR-215833; http://www.llnl.gov/tid/lof/documents/pdf/325503.pdf, October 2005.
[6] S. P. Hau-Riege, R. A. London, R. M. Bionta, M. A. McKernan, S. L. Baker, J. Krzywinski, R. Sobierajski, R. Nietubyc, J. B. Pelka, M. Jurek, L. Juha, J. Chalupsky, J. Cihelka, V. Hajkova, A. Velyhan, J. Krasa, J.Kuba,K. Tiedtke, S. Toleikis, T.Tschentscher, H. Wabnitz,M. Bergh, C. Caleman,K. Sokolowski-Tinten, N. Stojanovic, and U. Zastrau, "Damage threshold of inorganic solids under free-electron-laser irradiation at 32.5 nm wavelength," *App. Phys. Lett.* **90**, 173128 (2007)
[7] T. J. McCarville, P. M. Stefan, B. Woods, R. M. Bionta, R. Soufli, M. J. Pivovaroff, "Opto-mechanical design considerations for the Linac Coherent Light Source X-ray mirror system", Proc. SPIE **7077** (this Conference Proceedings).
[8] D. L. Windt, "topo - surface topography analysis", available at http://www.rxollc.com/idl/index.html
[9] G. M. Blumenstock and Ritva A. M. Keski-Kuha, "Ion-beam-deposited boron carbide coatings for the extreme ultraviolet", Appl. Opt. **33**, 5962-5963 (1994).
[10] G. M. Blumenstock, R. A. M. Keski-Kuha, and M. L. Ginter, "Extreme ultraviolet optical properties of ion-beam-deposited boron carbide thin films", Proc. SPIE **2515**, 558-564 (1995).
[11] C. Tarrio, R. N. Watts, T. B. Lucatorto, J. M. Slaughter, and C. M. Falco, "Optical constants of *in situ*-deposited films of important extreme-ultraviolet multilayer mirror materials", Appl. Opt. **37** 4100-4104 (1998).

[12] J. I. Larruquert and R. A. M. Keski-Kuha, "Optical properties of hot-pressed B4C in the extreme ultraviolet", Appl. Opt. **39**, 1537-1540 (2000).
[13] R. Soufli, R. M. Hudyma, E. Spiller, E. M. Gullikson, M. A. Schmidt, J. C. Robinson, S. L. Baker, C. C. Walton, and J. S. Taylor "Sub-diffraction-limited multilayer coatings for the 0.3 numerical aperture micro-exposure tool for extreme ultraviolet lithography", Appl. Opt. **46**, 3736-3746 (2007).
[14] R. Soufli, A. L. Aquila, F. Salmassi, M. Fernández-Perea, E. M. Gullikson, "Optical constants of magnetron sputtered boron carbide thin films from photoabsorption data in the range 30 to 770 eV", Appl. Opt. **47**, 4633-4639 (2008).
[15] D. G. Stearns, "A stochastic model for thin film growth and erosion," Appl. Phys. Lett. **62**(15), 1745-1747 (1993).
[16] E. Spiller, S. Baker, E. Parra, and C. Tarrio, "Smoothing of mirror substrates by thin film deposition," Proc. SPIE **3767**, 143-153 (1999).
[17] R. Soufli, E. Spiller, M. A. Schmidt, J. C. Robinson, S. L. Baker, S. Ratti, M. A. Johnson and E. M. Gullikson, "Smoothing of diamond-turned substrates for extreme-ultraviolet illuminators", Opt. Eng. **43**(12), 3089-3095 (2004).
[18] J. H. Underwood, E. M. Gullikson, "High-resolution, high-flux, user friendly VLS beamline at the ALS for the 50-1300 eV energy region," J.Electr. Spectr. Rel. Phenom. **92**, 265-272 (1998).
[19] E. M. Gullikson, S. Mrowka, B. B. Kaufmann, "Recent developments in EUV reflectometry at the Advanced Light Source," Proc. SPIE **4343**, 363-373 (2001).
[20] D. L. Windt, "IMD: Software for modeling the optical properties of multilayer films," Computers in Physics **12**, 360–370, 1998. Available at http://www.rxollc.com/idl/index.html